NMR Analyses of Order and Dynamics in Poly(*p*-Benzamide)/Sulfuric Acid Solutions

Min Zhou, Veronica Frydman, and Lucio Frydman*

Department of Chemistry (M/C 111), University of Illinois at Chicago, 845 West Taylor Street, Chicago, Illinois 60607-7061

Received February 20, 1997; Revised Manuscript Received June 23, 1997[⊗]

ABSTRACT: Natural abundance NMR methods were employed to analyze static and dynamic properties of poly(*p*-benzamide), the parent compound of the aramide family of polymers, dissolved in absolute sulfuric acid. Quantitative determinations of order in the liquid crystal phases arising in these systems were carried out with the aid of bidimensional ^{13}C NMR data collected in the solid phase and of total line shape simulations, and the parameters thus obtained were monitored as a function of temperature, concentration, and polymer molecular weight. These measurements revealed that by contrast to what had been inferred from previous macroscopic order determinations, the alignment of polymer molecules in their nematic domains is essentially independent of temperature. Existing measurements can still be explained in terms of a temperature-dependent isotropic ⇄ nematic equilibrium, whose presence and thermodynamics were unambiguously characterized by NMR. Dynamic aspects of this interphase equilibrium as well as of the intraphase molecular diffusion in the nematic region were explored by bidimensional and pulsed-gradient NMR methods. Spectroscopic results were analyzed in terms of thermal and athermal theories predicting the appearance of nematic phases in rigid anisometric polymers and compared with recent NMR observation on other lyotropic aramide solutions.

1. Introduction

The isotropic/nematic transitions that can arise upon dissolving certain natural and synthetic macromolecules in suitable solvents constitute the target of active theoretical and experimental research.[1−9] Interest in understanding the behavior of these liquid crystalline solutions is driven in part by the unusual properties that they display, as well as by the important roles that they play as precursors of materials possessing unique nonlinear optics and ultrastrong characteristics. Among the first and most successful class of macromolecules leading to these phases that were synthesized are the aramides, stiff aromatic polyamides whose processing exploits their tendency to generate liquid crystalline dopes when dissolved in strong mineral acids at appropriate concentrations.[10−13] A large number of liquid crystalline polymers have been synthesized over the last decades, including two that have become of commercial interest: poly(*p*-benzamide) (PBA, **1**), which can be

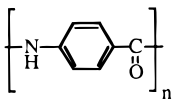

1

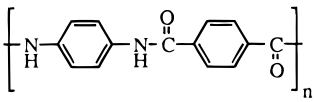

2

considered as the parent compound of the aramide family, and poly(*p*-phenyleneterephthalamide) (PPTA, **2**), the polymer from which the Kevlar and Twaron brands of commercial fibers are spun.

A common characteristic shared by these and other aromatic polyamides and polyesters is a long solution-phase persistence length, arising as a consequence of the highly conjugated and semirigid nature of their monomeric constituents. When combined with a marked molecular anisometry, this feature leads to solutions where the macromolecules behave as long rigid rods, capable of spontaneously orienting within a nematic domain when driven by appropriate enthalpic or entropic forces. These ordered microscopic arrangements can be further aligned by the application of external fields such as those generated upon flow, leading to oriented macroscopic fluids whose coagulation results in highly ordered solid structures. In view of these considerations it is easy to understand the importance that a better understanding of the static and dynamic properties adopted by macromolecules in these solutions can play in the processing of their final materials. Particularly relevant is the characterization and rationalization of the mode by which structural characteristics such as polymer molecular weight and chemical composition influence the molecular alignment within the nematic domains, as well as the way by which order is affected by controllable environmental factors such as temperature and polymer concentration. Also important is the characterization of inter- and intradomain diffusion processes, as these dynamic molecular phenomena play important roles in defining rheological properties of the solutions that can in turn influence the textures adopted by the final materials. The quantitative measurement and analysis of these static and dynamic properties in PBA/H_2SO_4 solutions is the main focus of the present investigation.

Numerous characterizations of the solid ⇄ nematic ⇄ isotropic equilibria that arise in PBA solutions have appeared in the literature. The majority of these measurements involved bulk calorimetric, solubility, optical, and rheometric analyses of the polymer dissolved in *N*,*N*-dimethylacetamide/LiCl,[11,14−18] while fewer studies focused on bulk optical, rheological, and susceptibility determinations of the polymer dissolved in absolute sulfuric acid.[19,20] We decided to focus the present investigation on the properties displayed by the latter solutions, as sulfuric acid is the solvent normally employed in the industrial processing of aramides.[13] Our experimental studies were based on nuclear magnetic resonance (NMR), a method whose capability to monitor molecular level properties of both solvent and solute in low molecular weight liquid crystals is well established.[21] In order to quantify the polymer order in the nematic phase, we relied mainly on natural abundance

[⊗] Abstract published in *Advance ACS Abstracts,* August 15, 1997.

S0024-9297(97)00233-7 CCC: $14.00

Scheme 1

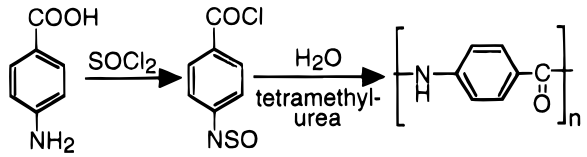

^{13}C NMR and interpreted these results with the aid of static tensor parameters measured for the polymer in the solid by isotropic−anisotropic 2D ^{13}C NMR spectroscopy. These measurements revealed an unexpected independence of PBA's order parameter on temperature and molecular weight, factors which did, however, affect the relative abundance of the isotropic and nematic phases in the solution. Our measurements also revealed a dependence of both the phase equilibria as well as the nematic order parameters on the polymer's concentration. When considered in unison, these features fail to support enthalpic models that describe aramide solutions on the basis of anisotropic intermolecular interactions but are in qualitative agreement with theories predicting the onset of liquid crystallinity on the basis of entropic considerations. Bidimensional exchange and gradient-based NMR techniques were also employed to extract information about the rates of inter- and intraphase molecular diffusion. The values measured for the former were considerably low, while the latter provided evidence for a substantial decoupling between the environments felt by solvent and solute in the liquid crystalline phase.

2. Experimental Section

PBA samples employed in this study were synthesized via the (sulfinylamino)benzoyl chloride route described by Kwolek *et al.* (Scheme 1)[11,22] and were subsequently characterized by elemental analysis (Midwest Microlab, Indianapolis, IN). Average polymer molecular weights M_w were estimated from intrinsic viscosity determinations in 96% H_2SO_4 at 25 °C using the Mark−Houwink relation $[\eta] = 1.9 \times 10^{-7} M_w^{1.7}$ reported by Schaefgen *et al.*[15] According to these measurements, the initial average weight of all batches that were analyzed here by NMR fell in the 10−11K range. In order to prepare the PBA solutions, aliquots of H_2SO_4 with titles in the (100.0 ± 0.3)% range were prepared by mixing adequate amounts of concentrated and fuming (10% free SO_3) sulfuric acid (Aldrich). Solutions with well-defined % w/w polymer concentrations were then obtained by independently weighing the PBA and the acid, and subsequently mixing these components with a mechanical stirrer for 24 h. This procedure was carried out inside a 10 mL sealed glass container that was itself placed inside an ice/water bath to prevent sample degradation.[22] For solute concentrations exceeding 13% w/w the resulting polymer dopes showed strong stirring opalescence, a characteristic of the onset of liquid crystallinity in aramide solutions.[10]

To carry out the spectroscopic determinations, aliquots were extracted from freshly made polymer solutions using custom-made glass syringes and inserted inside 5 mm NMR tubes that were subsequently sealed. The inherent viscosities of these PBA/H_2SO_4 solutions, suitably diluted with 96% H_2SO_4, were also measured before and after the NMR experiments in order to check for sample degradation. A negligible decrease in $[\eta]$, from 1.4 to 1.3 dL·g^{-1}, was observed while NMR experiments were carried out at or below 45 °C. When temperatures exceeded 45 °C, a substantial decrease in the solutions viscosities was noticed, and $[\eta]$ values as low as 0.4 dL·g^{-1} were determined for samples that had been subjected to temperatures exceeding 60 °C for long periods of time. This is an indication that a temperature-activated degradation of the macromolecular chain occurred in absolute H_2SO_4, and even though this process placed an upper limit to the temperature range at which intact polymers could be studied, it provided us with a simple way of decreasing the average M_w and thus analyzing the latter's effects on the nematic behavior.

The majority of the NMR measurements that we carried out were performed at 7.1 T using a laboratory-built spectrometer with solution, solid state, and microimaging capabilities. Ancillary determinations were also performed at 4.7 and 9.4 T using commercial Bruker spectrometers and Nalorac probeheads. In all cases the polymer solutions were left inside the NMR magnetic field for several hours prior to the recording of their spectra in order to ensure full equilibration at the temperature of operation. Repetitive measurements showed that an average waiting period of 3 h was sufficient to achieve such a goal, as judged by the constancy and reproducibility in the positions and intensities of the different PBA resonances. The laboratory-built 7.1 T system used in the studies was controlled by a Tecmag digital pulse programmer and included two radio frequency and two imaging (audio) channels, all of them capable of delivering over 1 kW of power onto suitably tuned loads. Solution and liquid crystal NMR spectra were collected in this spectrometer using a doubly-tuned Cryomagnetics probe and a vertical spinning stack. The ^{13}C acquisitions employed waltz-16 ^{1}H decoupling (15 μs $\pi/2$ pulses) and no NOE enhancement in order to enable us to quantify the relative abundance of nematic and isotropic phases.[23] The pulse-gradient diffusion measurements were carried out using a laboratory-built probe incorporating Helmholtz and Maxwell imaging coil pairs whose characteristics were described elsewhere.[24] Variable-temperature operation in all these experiments was achieved by means of a stream of heating/cooling gas, whose temperature was set using a controller based on Omega components. Solid phase ^{13}C NMR spectra were acquired using a dynamic-angle-spinning doubly-tuned probe, employing cross-polarization (CP) and high-power decoupling with nutation fields in excess of 70 kHz.[25] The spinning module in this probe, a 7 mm Doty stator, was interphased to a Whedco motor and motor-controller system and enabled us to measure the static ^{13}C tensor parameters for each site in PBA by 2D isotropic−anisotropic correlation spectroscopy.[26] In both the solution and solid state ^{13}C NMR measurements an average of 3000 scans separated by 2 s relaxation delay were acquired in each unidimensional acquisition; 32 scans were employed for the ^{1}H observations. Chemical shifts throughout this work assumed $\delta_{TMS} = 0$ ppm and used benzene and adamantane resonances as references for the solution and solid phase spectra. The NMR chemical shifts for the isotropic and anisotropic fluid ^{13}C resonances are estimated accurate within ±0.1 and ±0.25 ppm, respectively; a ±0.1 ppm accuracy is estimated for the ^{1}H NMR peaks on the basis of repetitive measures.

3. Results

3.1. Concentration and Temperature Dependence of PBA/H_2SO_4 NMR Spectra. Figure 1 displays a series of room temperature ^{13}C NMR spectra recorded for PBA as a function of its relative concentration in H_2SO_4. The most salient change occurring in these spectra involves the appearance of a new set of NMR peaks, which emerges as PBA concentrations exceed about 10% w/w and becomes the sole spectral feature as the polymer's concentration increases beyond 13% w/w. At low concentrations the ^{13}C NMR spectrum of PBA presents five peaks positioned at 125.7, 131.5, 134.2, 139.6, and 173.2 ppm, which on the basis of substituent chemical shift effects can be assigned to aromatic carbons *ortho*, *metha*, *para*, and *ipso* to the −NH− substituent and to the carbonyl carbon, respectively. We ascribe the new peaks appearing in the 12.4% solution at 155, 160, 187, 205, and 216 ppm to chemical sites of polymer molecules in a nematic phase, whose positions are shifted from their dilute δ values due to the onset of anisotropic chemical shift contributions. Concentration-driven variations also appear in the ^{1}H NMR spectra of these solutions, which are in all

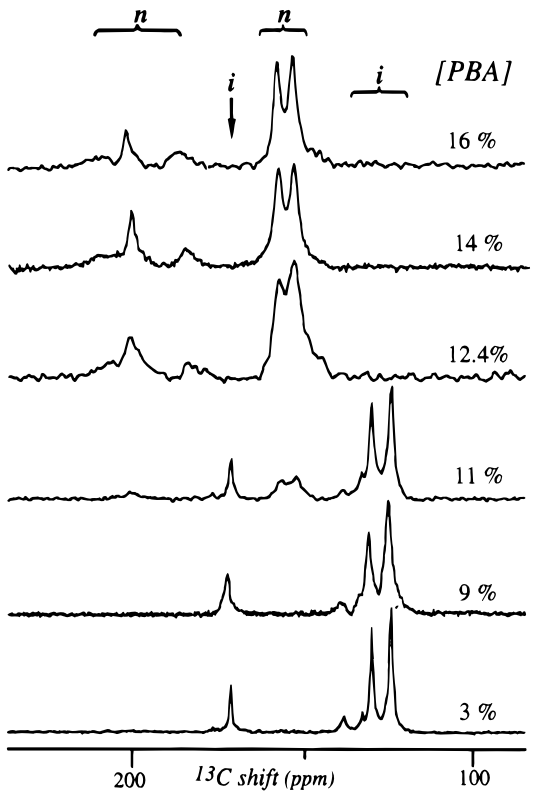

Figure 1. Dependence of the room temperature ^{13}C NMR spectrum of PBA/H_2SO_4 on polymer concentration. Letters i and n indicate resonances originating from molecules residing in isotropic and nematic phases.

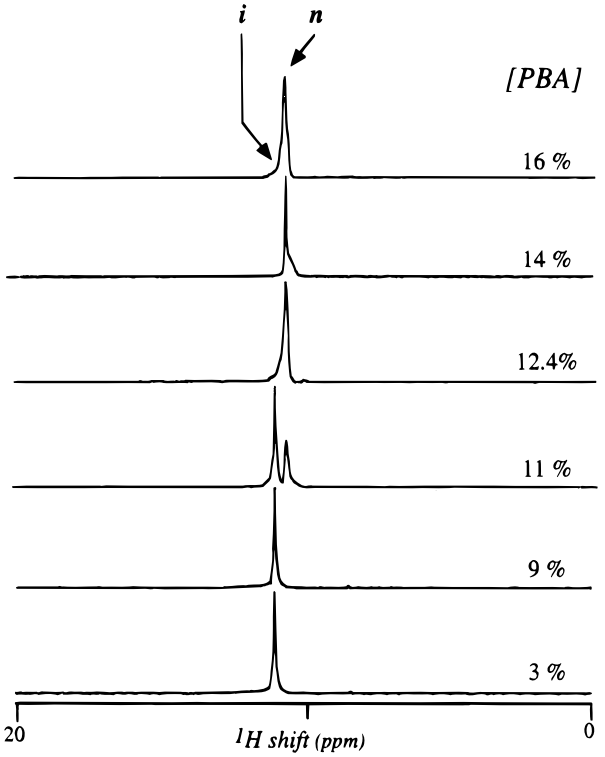

Figure 2. Concentration dependence of the room temperature ^1H NMR spectrum of PBA/H_2SO_4 solutions, showing peaks arising from solvent in either the nematic (n) or isotropic (i) phase.

cases dominated by the H_2SO_4 resonance (Figure 2). At low PBA concentrations this peak appears at 11.0 ppm, but as the polymer concentration increases, this resonance diminishes in intensity and a second peak at 10.6

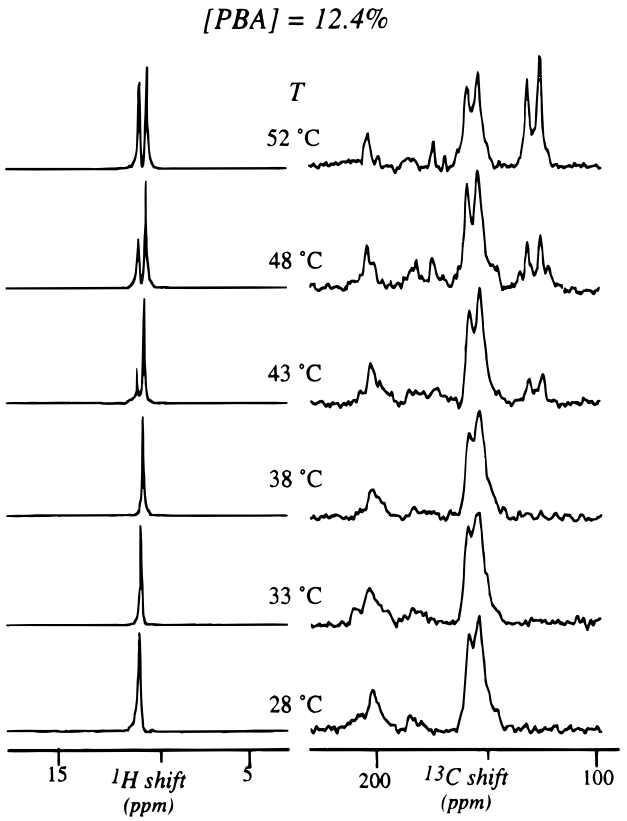

Figure 3. ^1H (left) and ^{13}C (right) NMR spectra of a 12.4% w/w PBA/H_2SO_4 solution recorded as a function of temperature. Spectral changes reflect variations in the isotropic ⇄ nematic equilibrium as viewed by solvent (left) and solute (right) molecules in the solution.

ppm emerges. The correlation between the changes occurring in these ^1H NMR traces and those appearing in the ^{13}C NMR spectra of the solute suggests that this new proton high-field peak arises from solvent molecules placed in the anisotropic phase; although the origin of the nematic shift experienced by this resonance is yet unclear, the absence of the expected anisotropic dipole−dipole splittings in this peak is likely to be a consequence of fast intermolecular proton migrations.

These ^1H and ^{13}C NMR spectral changes are reminiscent to the ones that have been recently reported for PPTA/H_2SO_4 solutions,[27] and as was the case with the latter, all changes can be reversed by dilution of the concentrated PBA solutions with pure H_2SO_4. Qualitatively similar changes to those shown in Figures 1 and 2 can also be observed in the ^1H and ^{13}C NMR spectra of PBA/H_2SO_4 solutions, when recorded at a single concentration but as a function of temperature (Figure 3). An important difference between these variable-temperature ^{13}C NMR spectra and the variable-concentration ones depicted in Figure 1 lies in the fact that anisotropic displacements in the former are essentially constant while in the latter they undergo measurable shifts; the meaning of these features is further discussed below.

Before proceeding to the quantification of these data it is worth evaluating how the spectral changes that are detected by NMR compare with the picture available about PBA/H_2SO_4 phase equilibria from other, non-NMR methods. These analyses include electronic microscopy and polarization measurements reported by Papkov *et al.*, who monitored the transitions and textures of an 11K PBA sample dissolved in 98% sulfuric acid.[19] For solutions with concentrations in the 8−13%

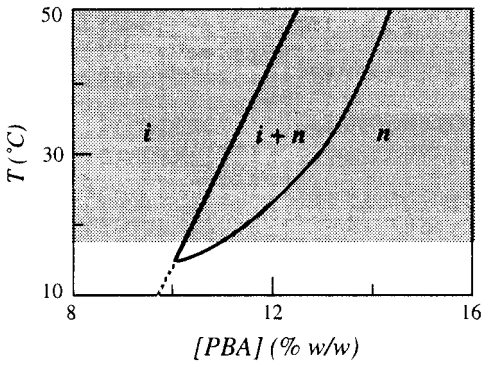

Figure 4. Schematic diagram describing the phase equilibria of PBA/H_2SO_4 solutions, with the shading illustrating the region explored in the present work. Abbreviations refer to isotropic (i) and nematic (n) phases.

w/w interval a nematic/isotropic phase coexistence was observed in the 20−60 °C region, ranges that are similar to the ones that we observe by NMR. Also in agreement with the NMR data, these analyses indicated an elevation in the T_{in} clearing temperatures as polymer concentrations increase, leading eventually to the appearance of solid particles whose signal we would not be able to detect under the present spectroscopic conditions. A more recent polarization microscopy study revealed qualitatively similar temperature and concentration dependences for the phase equilibria, albeit with clearing transitions occurring in the 40−100 °C range for 9−11% w/w PBA solutions.[28] These bulk PBA/H_2SO_4 studies, in combination with more extensive data available for other lyotropic polymers,[29] suggest that the changes observed in the NMR spectra can be understood on the basis of the phase diagram presented in Figure 4. The shaded area in this graph indicates the region that was explored in the present NMR study under the assumption that M_w, and thus the structure of the diagram, remained constant even at the highest temperatures.

3.2. Quantitative Analysis of Order in PBA/H_2SO_4 Solutions. In addition to qualitative phase coexistence information, the NMR spectra, and particularly the ^{13}C data, offer the possibility of quantifying the values and variations occurring in the nematic order parameter of the polymer throughout the various conditions. This information can be retrieved by analyzing the difference between PBA's chemical shifts when in the liquid crystal and the isotropic phases. Indeed, as macromolecules incorporate into a nematic they become aligned along a director and their isotropic tumbling ceases, endowing the various sites with an additional chemical shift displacement

$$\Delta\delta = \delta_{lc} - \delta_{iso} \tag{1}$$

due to the onset of anisotropic shielding contributions. These anisotropic displacements are best expressed in terms of the Saupe matrix $\{S_{ij}\}_{i,j=1-3}$, a second-rank tensor describing the relative degree of nematic order for each particular site, according to the equation

$$\Delta\delta = \frac{2}{3}\sum_{i,j=1-3} S_{ij}\delta_{ij} \tag{2}$$

The indices in this summation represent the directions of an arbitrary reference axis frame, and the $\{\delta_{ij}\}_{i,j=1-3}$ components denote the traceless ^{13}C shielding anisotropy tensor as described in the same frame of reference for the chemical site.

This expression can be further simplified for the case of rodlike lyotropics like PBA by considering the effective cylindrical symmetry adopted by these macromolecules in the fluid. This results in a negligible biaxiality ($S_{xx} - S_{yy}$) for the liquid crystalline phase and allows us to rewrite the anisotropic ^{13}C displacements in terms of a single order parameter S_{zz} defining the average order of the polymer chains with respect to the nematic director:

$$\Delta\delta = \frac{2}{3}S_{zz}\delta_{zz} \tag{3}$$

The chemical shift term δ_{zz} appearing in this expression denotes the anisotropic shielding component of a particular chemical site along the main polymer chain, once averaged over all the fast intramolecular motions taking place in the macromolecule. Equation 3 implies that order parameters for PBA can be extracted by a simple inversion of the experimentally measured liquid crystal displacements $\Delta\delta$, provided that the scaling factors δ_{zz} for the different chemical sites are known. A similar linear dependence of usually a single observable on S_{zz} is found when using other experimental approaches to nematic order determinations, including bulk polarization, rotatory, and susceptibility measurements.[30] An important advantage resulting from the use of NMR arises from the fact that the proportionality parameter δ_{zz} between molecular order and the observable shifts can be measured for the polymer itself using solid phase NMR techniques. This removes a potentially important source of inaccuracy from the estimation of order parameters; we discuss next how the individual δ_{zz} values for the different ^{13}C sites in PBA were established in this study.

The anisotropic chemical shift parameters δ_{zz} can be conveniently expressed in terms of the principal elements $\{\delta_{ii}\}_{i=1-3}$ defining individual shielding tensors and of second-rank Wigner matrices $\{\mathbf{D}^{(2)}_{m,m'}\}_{-2\le m,m'\le 2}$ describing the transformation undergone by these tensors upon undergoing a rotation.[31] For the particular case of anisotropic chemical shift displacements this parameter can be written as

$$\delta_{zz} = \sum_{l=-2}^{2} \langle \mathbf{D}^{(2)}_{l,0}(\Omega_{T\to D})\rho_{2,l}\rangle \tag{4}$$

where $\rho_{2,0} = (3/2)^{1/2}(\delta_{33} - \delta_{iso})$ and $\rho_{2,\pm 2} = (\delta_{22} - \delta_{11})/2$ are spherical tensor elements depending on the principal shielding tensor values, $\Omega_{T\to D}$ are Euler angles relating the tensor's principal axis system to the nematic director axis, and the brackets reflect the consideration of all rapid intramolecular motions. For a highly conjugated and stiff polymer like PBA it is natural to assume that these will only involve free rotations of phenyl groups about their *para* axes; a remaining dynamic possibility, involving elastic deformations of the macromolecules away from their main chain axes, is taken into consideration by the value resulting for S_{zz}. Because of this fast phenyl dynamics it is convenient to distinguish between the rotation matrices of the aromatic carbons, whose tensors will be averaged by the rotations, and those of the carbonyl ^{13}C tensor that will not. For the former the dynamic averaging can be

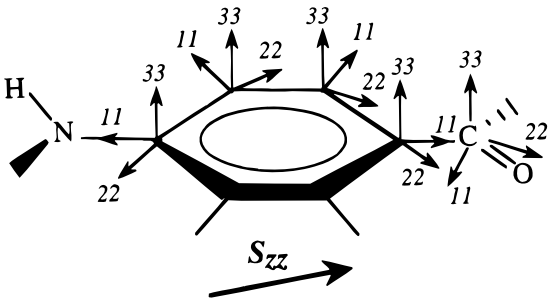

Figure 5. Orientations assumed by the principal axes shielding systems of the various ^{13}C sites in PBA. The directions of the $(ii)_{i=1-3}$ axes correspond with the $(\delta_{ii})_{i=1-3}$ components in Table 1; S_{zz} describes the orientation of the nematic director, parallel to the main macromolecular axis. On the basis of X-ray determinations,[33] we assume that the *para*-axes are tilted from the main polymer chain by 11°.

described by the series of successive rotations

$$\langle \mathbf{D}^{(2)}_{l,0}(\Omega_{T\to D})\rangle = \left\langle \sum_{n=-2}^{2}\sum_{m=-2}^{2} \mathbf{D}^{(2)}_{n,0}(\Omega_{R\to D})\mathbf{D}^{(2)}_{m,n}(\Omega_{R})\mathbf{D}^{(2)}_{l,m}(\Omega_{T\to R})\right\rangle \quad (5)$$

where $\Omega_{T\to R}$ denote the transformation of each tensor into a common reference frame whose z direction coincides with the axis of free phenyl rotations (the *para*-axis), $\Omega_R = (\varphi,0,0)$ describes the effects of free phenyl rotation, and $\Omega_{R\to D}$ transforms the resulting rotationally averaged tensors into the main axis of the nematic director. Whereas eq 5 needs to be integrated over the whole $0 \le \varphi \le 2\pi$ interval, no such averaging is required for the carbonyl tensor, whose rotation can still be described for the sake of consistency as

$$\langle \mathbf{D}^{(2)}_{l,0}(\Omega_{T\to D})\rangle = \sum_{n=-2}^{2} \mathbf{D}^{(2)}_{n,0}(\Omega_{R\to D})\mathbf{D}^{(2)}_{l,n}(\Omega_{T\to R}) \quad (6)$$

For all carbon sites we assume $\Omega_{R\to D} = (0,11°,0)$, as 11° is the angle resulting between the *para* phenyl axes and the main polymer chains when the latter are in the preferred all-*trans* configuration. The individual $\Omega_{T\to R}$ sets are defined by the polar (θ,φ) coordinates that describe the phenyl *para* axis in the principal axis system of each chemical shift tensor, which when dealing with planar moieties possessing local symmetry elements like phenyl and carbonyl groups can be accurately placed on the basis of extensively documented literature guidelines.[32] This literature information was employed in the present analysis, and the resulting orientations defining the $\Omega_{T\to R}$ sets for the different PBA sites are described in Figure 5 and Table 1.

Literature parameters could also be employed to estimate the approximate values of $\{\delta_{ii}\}_{i=1-3}$ for each site, but the much larger variability exhibited by these parameters would then limit the accuracy of our S_{zz} estimations to ca. ±10%. A more accurate alternative consists of measuring these tensor elements from the characteristic patterns that they originate in static powder ^{13}C NMR spectra.[25,34] Although the large line widths characterizing these NMR powder patterns would prevent their individual resolution from a conventional 1D spectrum of PBA, this limitation can be bypassed with the aid of more modern bidimensional (2D) NMR approaches. Particularly useful are 2D isotropic−anisotropic correlation methods, capable of separating the anisotropic powder patterns that will

Table 1. Values and Relative Orientations of PBA's ^{13}C Chemical Shift Tensor Parameters[a]

site	δ_{iso} (ppm)	δ_{11} (ppm)[b]	δ_{22} (ppm)[b]	δ_{33} (ppm)[b]	θ (deg)[c]	φ (deg)[c]
C=O	166	249	158	91	90	48
C–N	141	255	144	24	90	0
C–C	129	217	150	20	90	0
	127	219	162	−1	90	60
	122	207	156	3	90	60

[a] Isotropic solid phase shifts considered accurate within 1 ppm; individual tensor values accurate within ±3 ppm. [b] Under the convention δ_{11} = most deshielded element; δ_{33} = most shielded element. [c] Polar (θ) and azimuthal (φ) angles defining the relative orientation of the phenyl *para*-axis with respect to the individual principal axis tensor frames (δ_{11}||11, δ_{33}||33 in Figure 5).

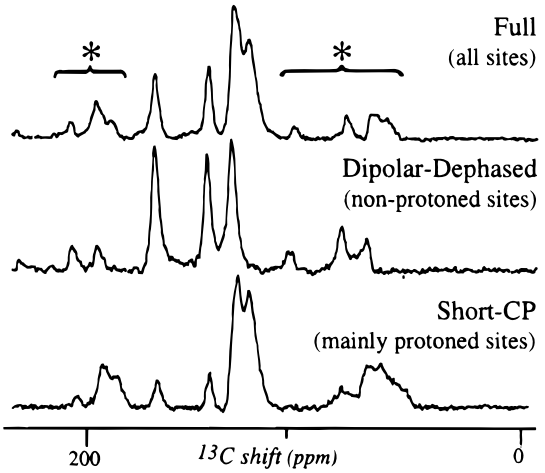

Figure 6. High-resolution solid state ^{13}C NMR spectra of powdered PBA collected using a 3 ms CP time (top, 500 scans), a 3 ms CP followed by 60 μs of dipolar dephasing for suppressing protonated carbons (center, 3000 scans), and a short (70 μs) CP time for enhancing almost exclusively the protonated carbons (bottom, 3000 scans). The last two strategies enable the separate NMR observation of all five ^{13}C sites in the monomer. Asterisks indicate spinning sidebands arising at multiples of the spinning frequency (≈5.2 kHz).

arise from different sites in a sample according to the isotropic chemical shift of each site.[26,35−38] Among the different techniques that can be employed for retrieving this kind of information we selected here the variable-angle correlations spectroscopy (VACSY) protocol, a particularly simple and sensitive experiment that is described elsewhere in detail.[26,39]

Even with this additional resolution enhancement technique site overlap remained a problem that needed to be dealt with in solid phase PBA determinations. This can be appreciated from the top trace in Figure 6, which shows the conventional 1D high-resolution ^{13}C NMR spectrum of polycrystalline PBA. Although this trace presents clear analogies with the isotropic solution spectrum recorded in H_2SO_4 (Figure 1, bottom), the additional line width created by sample heterogeneities and residual anisotropies prevents the resolution of all five inequivalent sites in the monomer. In order to bypass this limitation we decided to employ dipolar-dephasing and short-CP editing sequences,[40,41] techniques which can yield individual subspectra containing

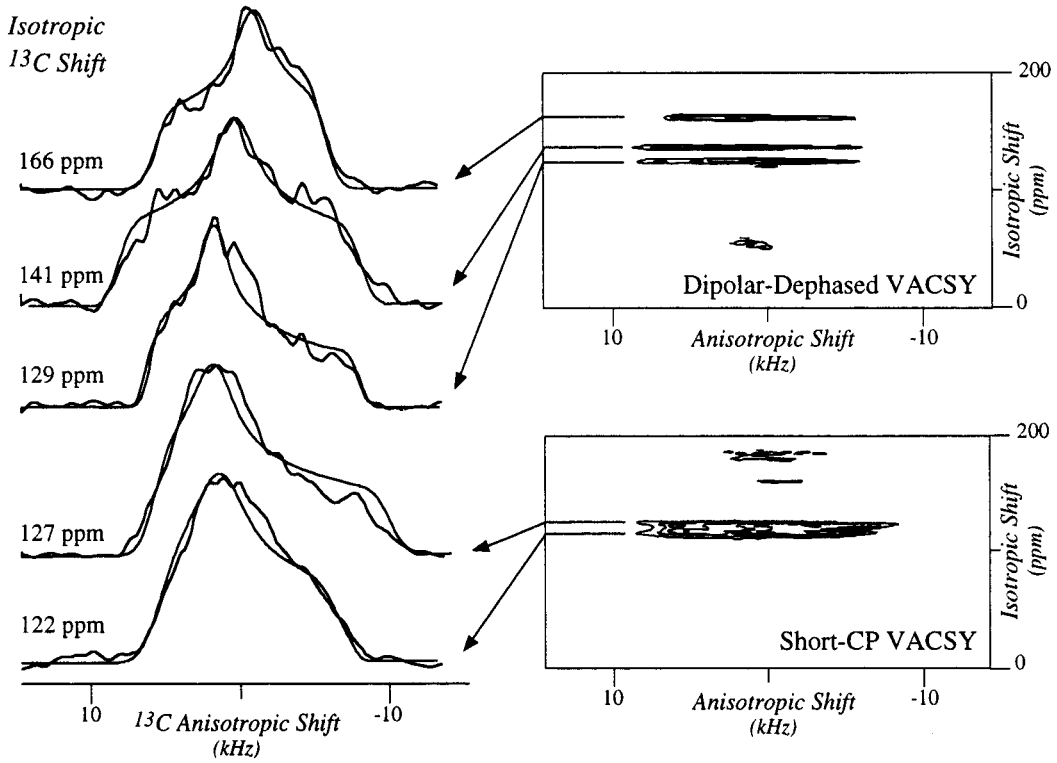

Figure 7. Summary of 2D VACSY NMR results obtained upon applying the dipolar-dephasing sequence (top) and the short-CP sequence (bottom) on polycrystalline PBA. On the right are the 2D VACSY spectra shown as contour plots; on the left are the anisotropic slices extracted at the indicated isotropic shifts. Superimposed on these experimental traces are best fit powder line shapes computed using the $(\delta_{ii} - \delta_{iso})_{i=1-3}$ components listed in Table 1. Experimental VACSY spectra are the result of 31 variable-angle acquisitions within the [90°, 35°] range, processed as described in ref 26.

the now resolved resonances of quaternary and protonated polymer carbons (Figure 6, center and bottom). In spite of the relatively poor signal-to-noise ratio characterizing these editing pulse sequences, they could still be combined with the VACSY procedure owing to the high efficiency of the latter experiment; the ^{13}C NMR data that the short-CP and the dipolar-dephased VACSY acquisitions then yield for PBA are summarized in Figure 7. The five powder line shapes that could be resolved in this manner were fitted with idealized powder distributions, which then complete all the shielding information that was required for calculating the individual δ_{zz} values (Table 1).

Equipped with this information, we set out to analyze the order parameters exhibited by PBA solutions at the various temperatures and concentrations by means of simulations of their total ^{13}C NMR line shapes. The approach that we employed in these simulations assumed that each chemical site in the polymer contributes isotropic and anisotropic Lorentzian line shapes $L(\delta - \delta_0)$ to a total site's spectrum, according to

$$I^{site}(\delta) = I_0^{site}\{x_{iso}L(\delta-\delta_{iso}^{site}) + x_{lc}L[\delta-\delta_{lc}^{site}(S_{zz})]\} \quad (7)$$

where x_{iso} and x_{lc} are the relative fractions of molecules in the isotropic and liquid crystalline phases, common to all sites in the polymer, and the scaling factor I_0^{site} takes into account the relative abundance of a particular site. The line widths of the two Lorentzians were assumed equal and set to the value that was experimentally measured for each site in the isotropic spectrum, a choice that became necessary in view of the nearly identical relaxation times that were measured for the resonances of the individual sites in both phases (Table 2). In order to reconcile this feature with the markedly larger line widths observed for all the ^{13}C nematic peaks as compared with their isotropic counterparts, a distribution in the order parameter S_{zz} was assumed. This distribution was modeled by a Gaussian function centered at S_{zz}^o and spread by a deviation ΔS_{zz},[27] and it is a reflection of heterogeneities in the polymer sample that will affect the overall alignment of the nematic director. The total ^{13}C NMR spectrum $I(\delta)$ observed at a particular temperature and concentration could then be simply calculated as a sum of individual subspectra

$$I(\delta) = \sum_{\text{all sites}} I^{site}(\delta) \quad (8)$$

This total line shape analysis presents a number of advantages when compared with more basic approaches of nematic investigation based on simple $\Delta\delta$ determinations. Two of them are its straightforward handling of multiple resonances and of cases of peak overlap, complications which arise in the ^{13}C NMR spectra of

Table 2. Relaxation Times of Selected ^{13}C PBA Resonances under Conditions of Nematic/Isotropic Coexistence[a]

chemical shift (ppm)	site	T_1 (ms)[b]	T_2 (ms)[b]
126	protonated aromatic, isotropic	130 ± 10	1.20 ± 0.30
131	protonated aromatic, isotropic	140 ± 10	1.25 ± 0.50
154	protonated aromatic, nematic	120 ± 20	0.90 ± 0.20
159	protonated aromatic, nematic	110 ± 20	1.15 ± 0.40
173	carbonyl, isotropic	470 ± 70	1.90 ± 0.70
205	carbonyl, nematic	450 ± 100	1.60 ± 1.00

[a] Determined from inversion-recovery and spin-echo data fits on 12.4% PBA solutions at 45 °C. [b] Error margins denote the standard deviations of the fits.

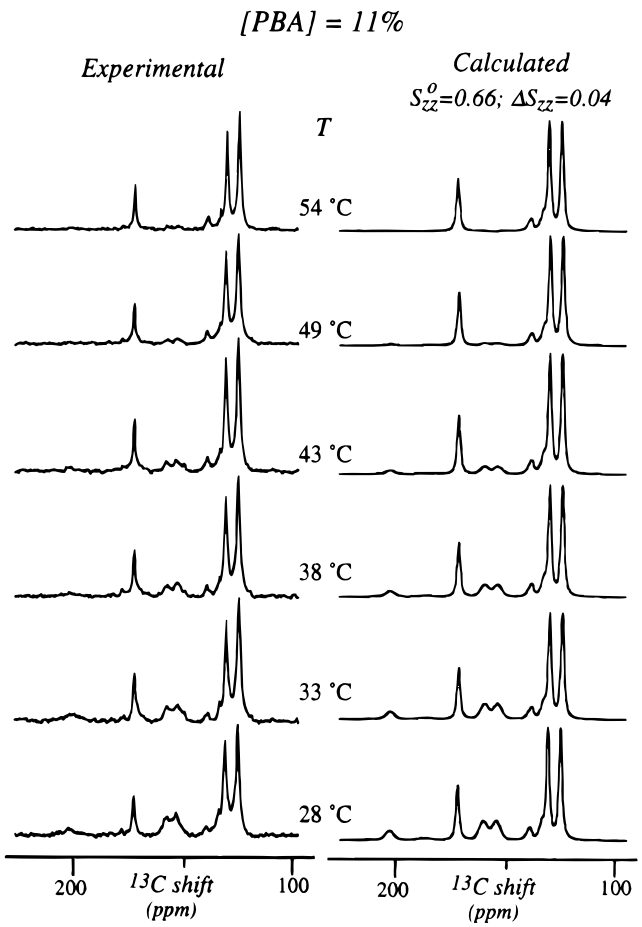

Figure 8. Comparison between experimental ^{13}C NMR spectra arising from an 11% w/w PBA/H_2SO_4 solution as a function of temperature (left), and best fit simulations calculated as described in the text using constant S^o_{zz} and ΔS_{zz} values while varying the x_{lc}/x_{iso} ratio (right).

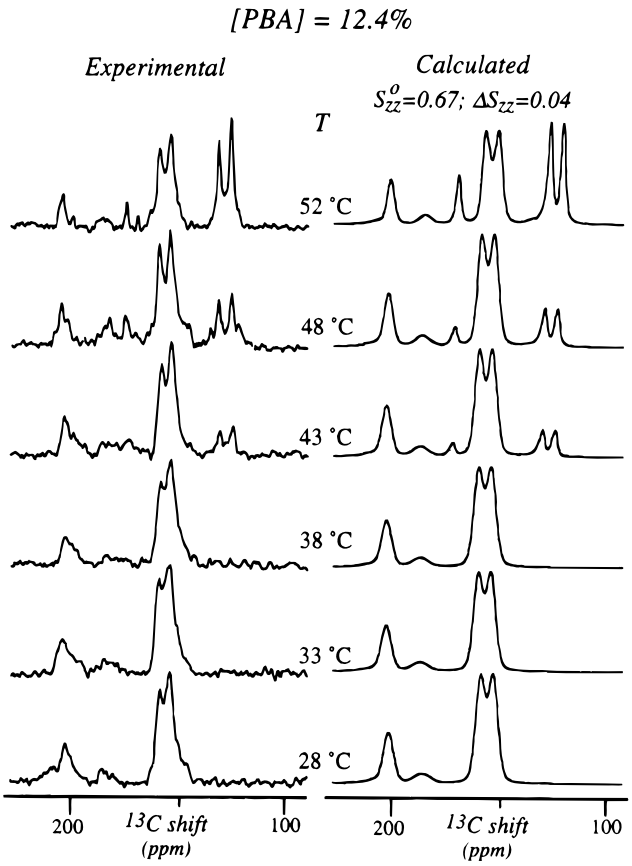

Figure 9. Same as Figure 8 but for a 12.4% w/w PBA/H_2SO_4 solution.

PBA. The method also has the advantage of simultaneously providing the relative abundance of the polymer in each phase (x_{lc}, x_{iso}) and the distribution ΔS_{zz} characterizing the nematic disorder. Furthermore, by virtue of the single order parameter that characterizes all sites in a rigid molecule like PBA and of the *a priori* determination of all tensor parameters by means of solid phase NMR, the total spectral line shape observed at each concentration and temperature will only depend on three independent parameters (x_{lc}, S^o_{zz} and ΔS_{zz}) whose effects on the simulations are highly distinctive. This in turn provides our determinations of average order with a high degree of accuracy, whose error we estimate at ±2.5% on the basis of repetitive data simulations.

With this formalism, the ^{13}C NMR data collected for 11, 12.4, 14, and 16% w/w PBA solutions as a function of temperature were analyzed; results arising from these experiments together with their corresponding simulations and calculated order parameter values are presented in Figures 8−11. In all cases the agreement between the observed and calculated behavior was excellent, with peak maxima deviating within these spectra by amounts comparable to our experimental and referencing errors. With the aid of these line shape simulations, it becomes possible to ascribe the origin of the various nematic peaks; for the 12.4% PBA concentration the ^{13}C resonance appearing at 205 ppm corresponds to the carbonyl carbon, whereas peaks at 216, 187, 160, and 155 ppm correspond to phenyl carbons that are *ipso*, *para*, *metha*, and *ortho* to the −NH− substituent in the monomer, respectively. The changing peak intensities displayed by all sites in the ^{13}C NMR spectra in Figures 8−11 indicate a shift in the relative amounts of polymer dissolved in the liquid crystalline and isotropic phases. One way of interpreting these variations is by considering a phase diagram like the one illustrated in Figure 4, whose phase boundaries will provide the ratio between macromolecules in the nematic and isotropic phase for the different equilibria by application of the lever rule.[42] Alternatively, spectral changes can be viewed in terms of the equilibrium

PBA (isotropic phase) ⇄ PBA (liquid crystalline phase)

a dynamic process for which NMR clearly reveals a temperature dependence. Although the spectroscopic data do not provide a measure of the polymer's activities in each of these phases, the spectral simulations can yield, at least for those concentrations where the two phases coexist, a formal description of the constant defining this equilibrium in terms of the ratio $K_{eq} = x_{lc}/x_{iso}$. These ratios can in turn be exploited toward the construction of Van 't Hoff plots encoding the enthalpic and entropic parameters of the phase equilibrium (Figure 12). The pseudothermodynamic parameters resulting from this procedure are similar to the ones that were recently reported for the phase equilibria of PPTA/H_2SO_4 solutions.[43]

3.3. Dynamic Characteristics of PBA/H_2SO_4 Solutions. In addition to these static equilibrium properties, NMR can provide valuable information about the dynamic characteristics of PBA/H_2SO_4 solutions. Two

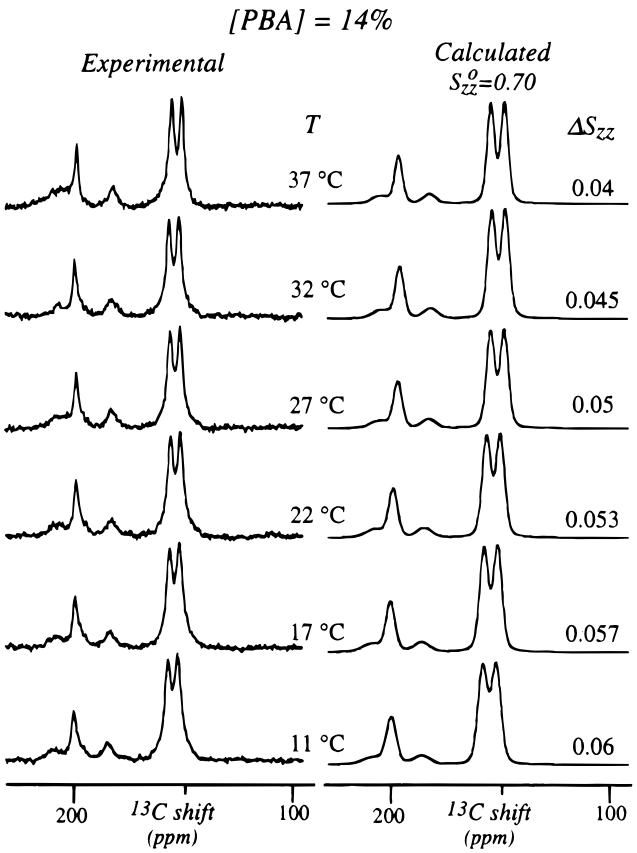

Figure 10. Variable-temperature ^{13}C NMR spectra of a 14% w/w PBA/H_2SO_4 solution (left). No isotropic peaks are visible under these conditions and no changes in the order parameter S_{zz}^{o} were apparent. Temperature variations of the peak line widths were taken into account in the simulations (right) by the indicated ΔS_{zz} values.

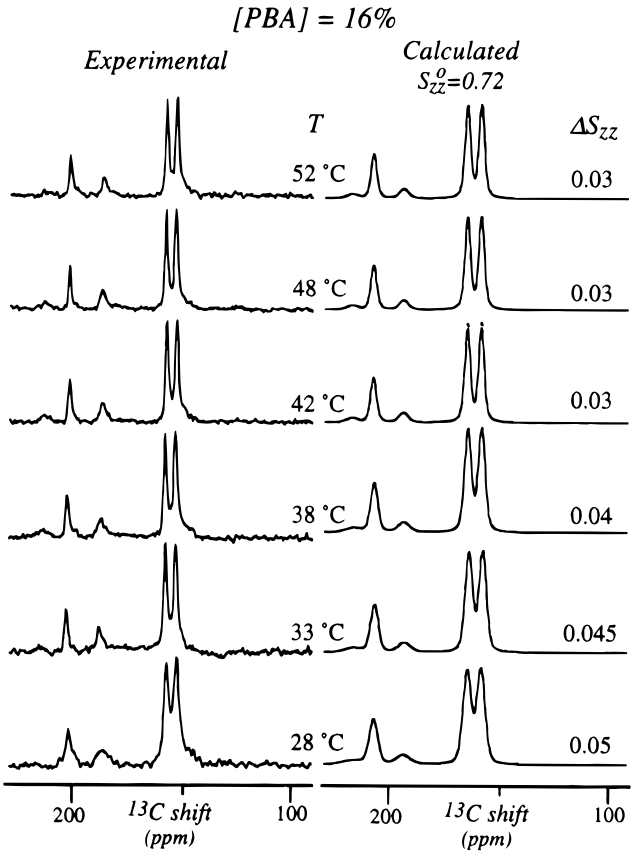

Figure 11. Same as in Figure 10 but for a 16% w/w PBA/H_2SO_4 solution.

aspects that we tried to address using NMR concerned the rates at which solute and solvent molecules exchange between the different phases in the region of nematic ⇄ isotropic coexistence, and the anisotropic character of the molecular diffusion within the aligned liquid crystalline phase. As mentioned earlier, these spontaneous molecular migration dynamics are related to the rheological properties of the solutions, which can in turn determine the development of structures and textures in aramides and in other liquid crystalline polymers after being processed.

Interphase PBA dynamics can be investigated using NMR by virtue of the coexistence, under certain concentration and temperature conditions, of well-resolved isotropic and nematic ^1H and ^{13}C resonances. The fact that for none of the samples did the ^1H or ^{13}C NMR spectra present even the onset of temperature-dependent exchange broadenings places an upper limit on the rate of molecular exchange between phases on the order of the frequency separation between the peaks ($10-10^2$ Hz).[23] An experiment capable of exploring this evidently slow rate of interphase migration is 2D exchange NMR,[44] a technique where chemical sites are monitored at two different times separated by a mixing period during which changes in their environment may take place. ^1H NMR results obtained when applying this approach to the solvent resonance under conditions of nematic/isotropic coexistence are illustrated in Figure 13. Although these contour plots present no evidence of dynamics for time scales shorter than 1 s, interphase cross peaks begin to emerge for longer mixing times, suggesting an average solvent lifetime in each phase

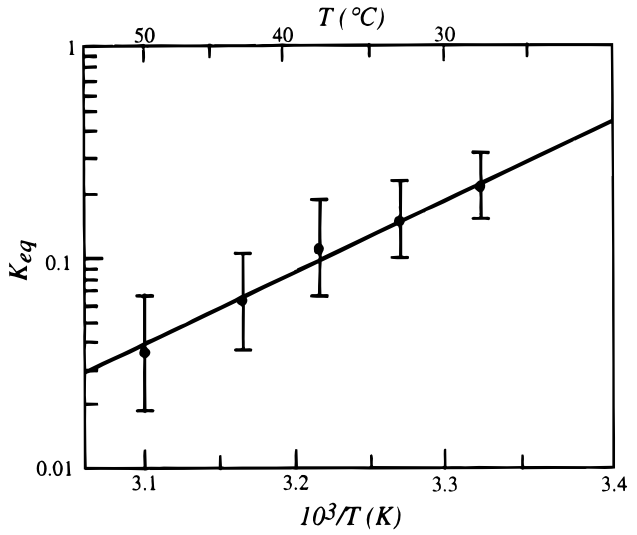

Figure 12. Van 't Hoff plot resulting from the x_{lc}/x_{iso} ratios employed in the variable-temperature simulations shown in Figure 8. The best fit of the data to the equation $K_{eq} = x_{lc}/x_{iso} = \exp(-\Delta H/RT)\exp(\Delta S/R)$ (line) yields $\Delta H = -(16 \pm 1)$ kcal·mol^{-1}, $\Delta S = -(57 \pm 6)$ cal·K^{-1}·mol^{-1}.

on the order of 10 s. When a similar approach was applied to investigate the behavior of the dissolved PBA polymer by ^{13}C NMR, no cross peaks could be observed at any of the assayed mixing times. In order to increase the sensitivity of our measurements an alternative dynamic NMR approach, the inversion-exchange method of Hoffman and Forsén,[45,46] was tested on these system. This technique, applicable to simple spectra such as those of PBA possessing few and well-resolved resonances, involves the selective inversion of one set of peaks (in our experiments the protonated nematic

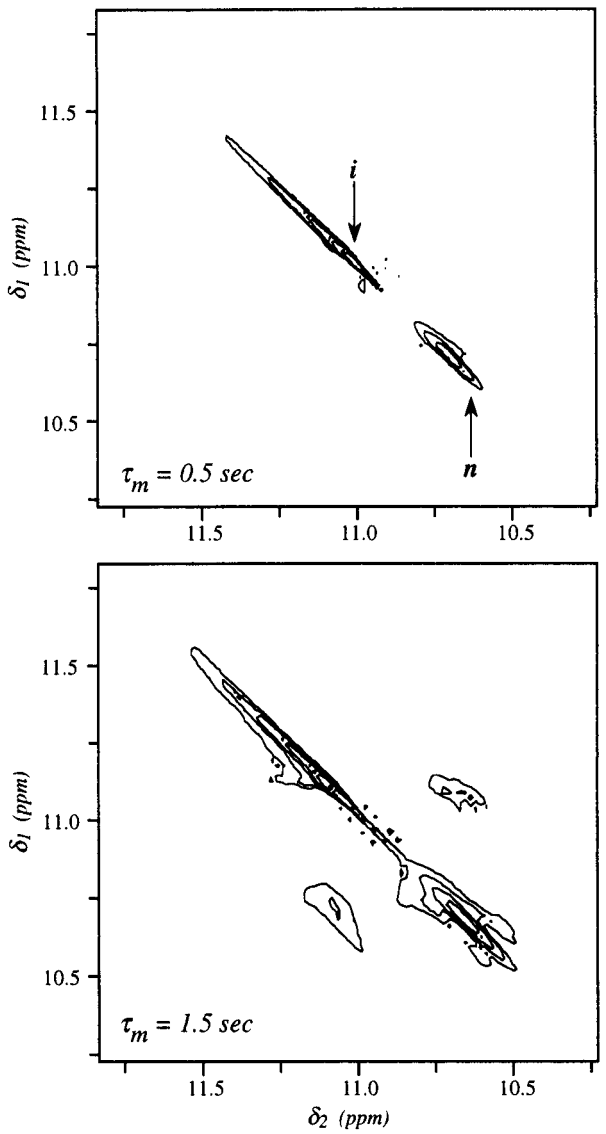

Figure 13. 2D ^{1}H-exchange NMR spectra arising from a 12.4% w/w PBA/H_2SO_4 solution at 48 °C for the indicated mixing times τ_m. Spectra are the result of 512 scans/t_1 point and 128 t_1 acquisitions; contours are geometrically spaced between 5 and 40% of the maximum peak intensity. Although the longest mixing time assayed in these experiments was comparable to the T_1 relaxation times of the H_2SO_4 peaks (ca. 1.0 s), no S/N complications were encountered owing to the strong intensities of these resonances.

carbons) followed by the observation of the peak intensities in potential exchange partners (the protonated isotropic carbon resonances) as a function of a mixing time. Figure 14 presents the ^{13}C NMR results obtained with this method on an 11% PBA/H_2SO_4 solution; the absence of any apparent changes in the isotropic signal intensities within the time scale allotted for observation by spin−lattice relaxation indicates that the lifetime of the solute in each phase is comparable if not longer than that of the solvent protons.

In addition to these interphase exchange measurements, NMR can be used to probe molecular diffusion within each phase of PBA by means of the pulsed-gradient spin-echo (PGSE) microimaging experiment. In this method molecular positions are encoded and decoded at two different times by the application of appropriate field gradients ±G, separated by a delay time during which displacements are allowed to occur. These motions will produce an attenuation of the NMR

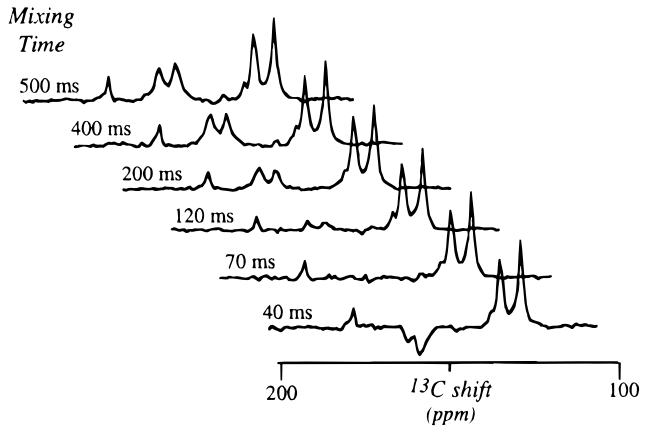

Figure 14. Inversion-exchange ^{13}C NMR spectra observed at room temperature for an 11% w/w PBA solution for the indicated mixing times. These experiments involved a DANTE-based 180° selective pulse on the nematic protonated resonances, followed by a mixing period and a final 90° observation pulse. The absence of variations in the isotropic signal intensities is indicative of negligible exchange over the indicated time scales.

signal that if monitored as a function of the gradient strength $|G|$, allows one to extract the diffusion coefficient along the G-direction.[47,48] Results obtained upon applying this technique to a purely nematic 14% w/w PBA solution are presented in Figure 15. Also shown in this figure for the sake of comparison are PGSE NMR results arising from variable-temperature measurements on concentrated H_2SO_4, and on a 16% w/w anisotropic solution of PPTA/H_2SO_4. In all cases the proton diffusivities in the polymer solutions were slightly slower than those observed in pure H_2SO_4. The alignment of polymer chains along the B_0 field also seems to favor the diffusion of H_2SO_4 protons in a direction that is parallel to the external magnetic field, although the $D_\parallel/D_\perp$ ratios for both the PPTA and PBA solutions are very close to unity. Unfortunately, the short spin relaxation times of PBA itself prevented us from recording similar high-quality ^{13}C PGSE NMR data from these solutions; ways of bypassing these signal-to-noise limitations are currently being sought.

4. Discussion

The preceding results provide ample evidence for the capability of natural abundance NMR to characterize the properties of PBA/H_2SO_4 solutions. Particularly promising is the possibility of accurately determining order parameters by ^{13}C liquid crystal NMR with the aid of coupling tensor elements measured for the polymer in the solid phase. The reliability of these ^{13}C NMR determinations can be appreciated from the fact that the resonance positions, line widths, and intensities of all carbon sites in all spectra could be simultaneously reproduced using well-defined and physically meaningful parameters. Among the previous studies that focused on PBA solutions at least two have also been concerned with the quantification of similar parameters in the nematic. In one of these studies, Ciferri and coworkers employed polarized IR techniques in order to analyze room temperature solutions of the polymer dissolved in dimethylacetamide/LiCl.[18] This study employed specially treated KBr cells as well as moderate (1 T) magnetic field strengths for inducing a macroscopic alignment of the nematic domains, and its data interpretation was based on IR parameters taken from model compounds. Room temperature order parameters in the

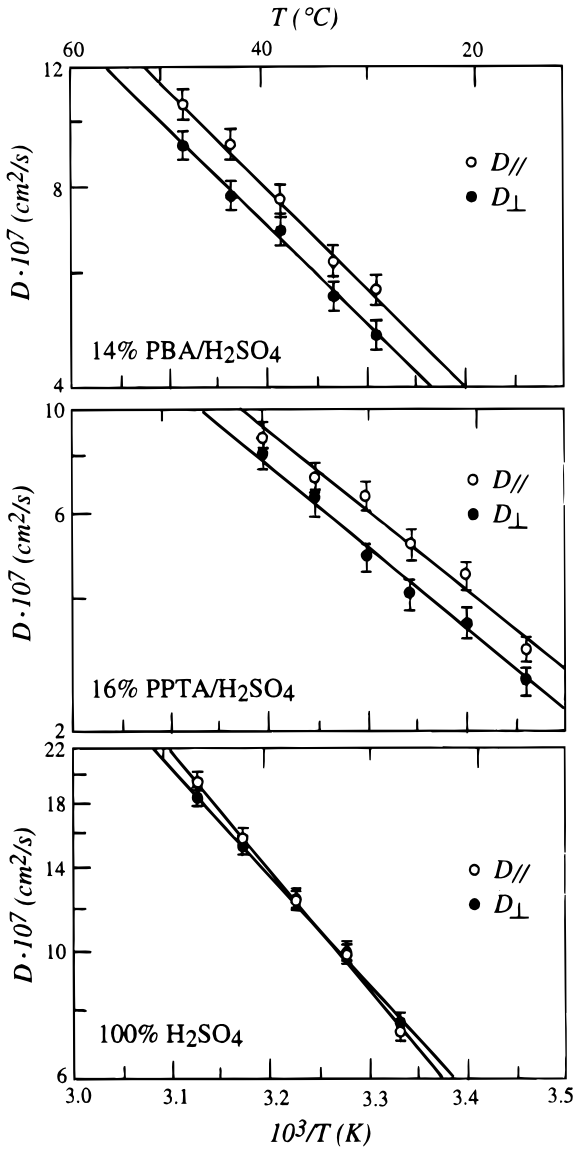

Figure 15. Diffusion coefficients ($D_{||}$, $D_{\perp}$) observed parallel and perpendicular to B_0 for the H_2SO_4 protons in the indicated solutions as a function of temperature. Values were calculated by fitting PGSE decay curves, whose acquisition involved 2 ms gradient pulses, 300 ms spin echo delays, and ten $|G|$ values distributed over the 0−100 kHz/cm range. No deviations from the ln (S/S_0) vs $|G|^2$ linearity could be detected in any of these decay curves. Straight lines in the plots correspond to least squares fits of the diffusion coefficients under the assumption that they follow a thermally-activated Arrhenius dependence; brackets denote the error intervals of the D coefficients as estimated from repetitive PGSE measurements.

0.76−0.83 range were thus determined, depending on the polymer concentration. These figures are slightly higher than the S^{o}_{zz} values that we observed by NMR (Figures 8−11), a difference which could easily originate in the different nature of the two PBA solutions.

Direct comparisons are feasible, however, between our ^{13}C NMR results and data reported in a recent depolarized light study of PBA/H_2SO_4 solutions.[20] Over temperatures and concentrations similar to the ones that we have analyzed here by NMR this bulk measurement technique afforded order parameters ranging between 0.44 and 0.88, an interval that includes but exceeds that of our observations. These optical results might be liable to a bias due to the fact that the anisotropy parameter ΔI_o scaling the experimental light depolarization, a factor analogous to the δ_{zz} term in eq 3, could not be independently measured and was thus estimated from theoretical considerations. Regardless of this scaling uncertainty, the depolarized light study shows an important discrepancy with our NMR results: it observes a strong temperature dependence for the order parameters of PBA/H_2SO_4 solutions. A similar temperature dependence had also been previously reported on the basis of microscopy measurements for other types of aramide/H_2SO_4 solutions, including PBA and PPTA.[7,28] In fact, this thermal dependence of the order parameter arises naturally from the Meier−Saupe mean field theory, a model that is frequently employed for explaining the appearance of nematic phases in liquid solutions.[49,50] According to this theory, extensively applied with success in the field of low molecular weight thermotropics,[30] nematic domains arise in the solutions of certain aromatic molecules due to their capability to feel and exert on their neighbors an orientation-dependent intermolecular potential. This anisotropy, which can be either attractive or repulsive,[51] leads to a nonrandom orientational distribution function of the form

$$f(\beta) = \exp \frac{[\epsilon S_{zz} P_2(\cos \beta)]}{kT}/Z \qquad (9)$$

where ϵ describes the strength of intermolecular interactions and Z is the partition function of the solution. The kT Boltzmann factor appearing in eq 9 is a clear indication that the nematic order parameters generated by this distribution function will be temperature dependent, even if they can be expected to be constant in the region of nematic/isotropic coexistence.[52]

In spite of the mutual consistency between these theoretical predictions and the thermal behavior reported by previous experiments, the ^{13}C NMR data presented in the preceding section unambiguously demonstrate that order parameters in PBA/H_2SO_4 solutions are temperature independent. This independence holds true at least within our relatively small range of experimental errors, and for the 11−16% w/w range of PBA concentrations that were studied. A more quantitative picture of this statement can be appreciated from Figure 16 (top), which presents the average changes occurring in the nematic displacements of PBA's protonated carbon peaks with temperature and concentration for the analyzed solutions. Notice that whereas the former factor introduces only minor and random changes, the latter produces unambiguous and systematic variations in the nematic chemical shifts of PBA. Furthermore, in an effort to compare our data with those previously obtained using bulk measurement techniques (which extended to ca. 90 °C), we have included in this variable-temperature plot points from high-temperature spectra even though our viscosity measurements indicate that under these conditions an onset of macromolecular degradation occurs. The lack of systematic variations in these ^{13}C nematic chemical shifts is therefore indicating that within the minimum ranges compatible with the onset of liquid crystallinity, order in PBA solutions is largely independent not only of temperature but also of the polymer's molecular weight. Similar conclusions could be reached from recent ^{13}C and ^{2}H NMR data collected on PPTA/H_2SO_4 solutions.[27,53] Also shown for the sake of completion in Figure 16 (bottom) are selected ratios between the nematic displacements observed for different PBA sites at various concentrations; by contrast to the behavior

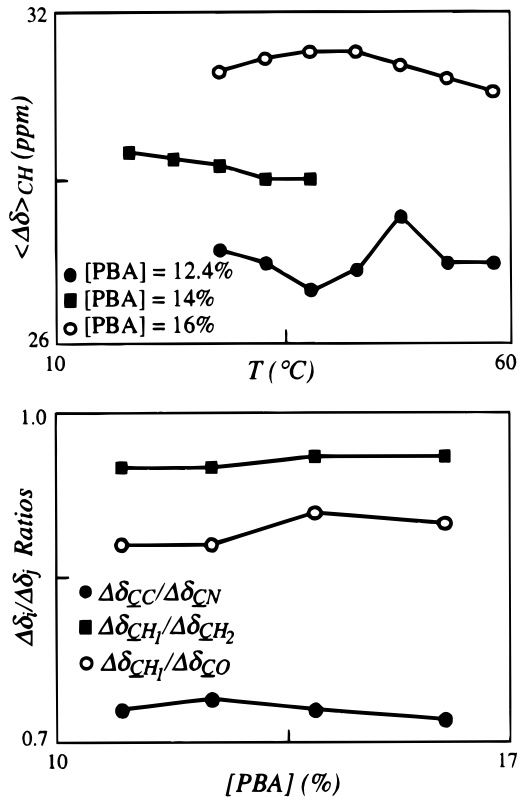

Figure 16. Top: Temperature and concentration dependence observed for the average anisotropic shifts $\langle\Delta\delta\rangle$ of protonated aromatic carbons in PBA/H_2SO_4 solutions. Bottom: Behavior observed for selected ratios between anisotropic ^{13}C shifts (underlined sites) at different concentrations and $T = 28$ °C. The constancy displayed by these plots is an indication of the validity of eq 3 and of the assumptions involved in its derivation.

shown by the absolute $\Delta\delta$ values, these ratios are essentially constant throughout the series, in correspondence with the prediction of eq 3.

In spite of this disagreement between the pictures inferred from the optical and NMR data, both sets of results can still be reconciled by virtue of the temperature-dependent equilibrium that the latter technique observes between the nematic and isotropic phases. Indeed, although previous studies based on bulk measuring techniques could not have distinguished between a decrease in the apparent nematic order parameter S^o_{zz} and a displacement of the nematic $\rightleftarrows$ isotropic equilibrium toward an isotropic phase, a molecular level probe like ^{13}C NMR unambiguously points toward the second of these possibilities. Still, before accepting this result and going through the relatively drastic step of discounting the applicability of the Meier−Saupe model to PBA/H_2SO_4 solutions, it might be worth considering the potential effects that the external NMR magnetic field could have had on our determinations of S^o_{zz}. This field, which enables our measurements by aligning the microscopic nematic domains into a macroscopic homogeneous ensemble, could also have been a perturbing factor whose constancy throughout the experiments was responsible for the constant S^o_{zz} values observed as a function of temperature and M_w. In order to explore this possibility, we repeated some of the experiments that were described in the preceding section as a function of B_0. Figure 17 illustrates a representative set of these variable-field ^{13}C NMR results and shows that no changes in PBA's anisotropic shifts occur upon

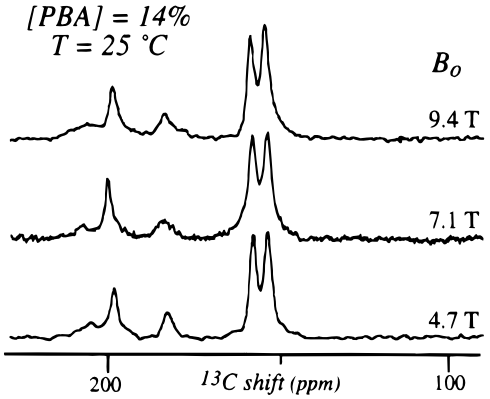

Figure 17. ^{13}C NMR spectra recorded for a 14% w/w PBA/H_2SO_4 solution at room temperature using the indicated magnetic field strengths.

varying the value of the external magnetic field between 4.7 and 9.4 T. This in turn implies that the magnetic field is not a determining factor in the values of S^o_{zz} that are observed by NMR and is merely an auxiliary aid for aligning *a priori* randomized nematic domains into a system with bulk macroscopic order.

In view of these results it is worth considering how another leading theoretical approach, this one based on Onsager's calculations on the behavior of hard rigid rods, compares with the liquid crystalline parameters that we observe in the PBA solutions. This model assumes that macromolecules exert on one another infinite repulsions if their structures overlap and negligible interactions otherwise, thereby leading to an athermal description of molecular order.[30,54] An approximate solution to the order parameter in the resulting model can be calculated from a virial expansion for the solute's molar free energy, which to first order can be expressed as

$$\frac{F}{N_A kT} = \frac{F^0}{N_A kT} + \ln[\text{solute}] - \Delta S_{\text{trans}} - \Delta S_{\text{or}} + \text{O}[\text{solute}]^2 \quad (10)$$

where the second term on the right represents an ideal mixing entropy and the third and fourth terms represent the loss in translational and orientational entropy resulting from the interactions between the hard-rod solute molecules. These three terms will depend on the molecular orientational distribution $f(\beta)$ adopted by the macromolecules, and an overall minimization of F predicts that beyond certain concentrations and length/diameter ratios, $f(\beta)$ will become anisotropic. An important difference between this model and the one underlying eq 9 lies in the fact that it predicts a temperature-independent but concentration-dependent order distribution, features that are in general agreement with the behavior observed by NMR for the PBA/H_2SO_4 solutions (Figures 8−11 and 16).

At a more quantitative level, however, the results of Onsager's approximation depart from the experimentally measured range of PBA's order values. A variational solution to eq 10 predicts minimum order parameters for infinitely long rods of 0.85, an S^o_{zz} value which decreases only slightly upon numerically solving Onsager's problem in an exact form.[55] Alternatively, Flory proposed a more accurate rendering of the repulsive rigid-rod problem that, on the basis of lattice models, bypasses Onsager's virial approximation.[56,57] Although

this approach can lead to exact orientational distributions for lyotropic solutions, it still overestimates the order that is observed for PBA and predicts a minimum S_{zz}^{o} value in the case of infinite rods of ca. 0.9. Of course, aramide solutions do not necessarily constitute ideal dispersions of infinite rigid rods subject to these simplified types of potentials, and additional parameters such as polydispersity, solute−solvent interactions, anisotropic attractive forces and macromolecular semiflexibility could also be important factors whose consideration has been deemed relevant for a proper description of nematic order in polymers.[6,53,58,59] Our NMR results, however, indicate that some of these variables play at most a minor role in the order characteristics of the nematic solute. For instance the independence that NMR reveals for the order parameters of PBA with respect to M_w in the 5−12 kg·mol^{-1} range suggests that polydispersity is not a defining factor in the value taken by S_{zz}, even if it will definitely affect the isotropic ⇄ nematic equilibrium at a given temperature. By contrast, macromolecular semiflexibility might play a more important role in explaining why the aramide order parameters that are observed by NMR are lower than the theoretical values derived from rigid rod theories. Indeed, even a simple "crankshaft" model, according to which aramides depart from their ideal all-trans conformation,[59,60] would endow these polymers with an additional degree of freedom, which when combined with rotational averaging, could reduce the ideal order parameters of the different sites. This additional averaging, which would be peculiar to *p*-phenylene macromolecules, could also explain why aramides have lower order parameters than other, more rigid, hydrogen-bonded lyotropic polymers such as PBLG.[61] It should be noted, however, that more modern theoretical models retaining higher-order virial coefficients or relying on scaled particle theories are also capable of predicting smaller order parameters than Onsager's and Flory's models,[6,8] which would then fall within the range that is experimentally observed for PBA.

Also worth discussing are the dynamic aspects of this work. Although our initial goal was to use NMR for determining a number of interesting and yet unknown properties of the dissolved polymer itself, such as phase lifetimes and diffusion coefficients, short ^{13}C spin relaxation times and long dynamic time scales conspired against these determinations. Our quantitative measures were therefore confined to observations of the solvent ^{1}H resonance. The diffusion coefficients measured for the solvent protons in nematic PBA/H_2SO_4 and PPTA/H_2SO_4 solutions by PGSE NMR were only slightly inferior to those characterizing pure H_2SO_4, and their anisotropic character was weak. If one were to reference the observed H_2SO_4 $D_{\parallel}/D_{\perp}$ ratios ($\leq$1.1) to similar ratios measured in low molecular weight liquid crystals[24,62] or to values numerically calculated for liquid crystalline polymers,[63,64] one would have to conclude from the larger values of the latter ($\approx$1.5−2) that there is only a weak coupling between the highly ordered polymer and its surrounding solvent. This weak coupling between solute and solvent is paralleled by the strong anisotropic NMR shifts that are observed for the former and with the negligible dipolar broadenings that affect the latter. Overall, these marked differences between solvent and solute behaviors indicate that the H_2SO_4 is a poor reporter on the anisotropic properties of the nematic aramide itself and that care should be exercised upon attempting to extract quantitative conclusions from bulk measurements that include strong solvent contributions.

5. Conclusions

The present work demonstrated the feasibility and advantages resulting from the use of natural-abundance NMR, and particularly ^{13}C NMR, for obtaining a molecular description of the isotropic ⇄ nematic equilibrium, the alignment, and the dynamics in PBA/H_2SO_4 solutions. The appearance of distinct resonances enabled us to monitor phase coexistence as a function of temperature, concentration, and molecular weight, observations that in combination with tensor parameters measured for the solid polymer provided an accurate characterization of the nematic under different conditions. In contradiction to the description that was available about this system from bulk macroscopic measurements these NMR results unambiguously showed that at least within the explored ranges of temperatures and molecular weights, order in PBA remains essentially constant. These factors will, however, have a marked effect on the amount of polymer incorporated into the nematic and isotropic phases, thus explaining the results afforded by the bulk measuring techniques. In view of these NMR observations one is led to the conclusion that the Meier−Saupe mechanism describing nematic order based on anisotropic intermolecular interactions is not well suited to the description of lyotropic PBA solutions. By contrast, the increase in S_{zz}^{o} with concentration that NMR revealed for the nematic lends support to Onsager's and Flory's athermal models of molecular alignment, even if an exact quantitative agreement between these theories and experiment still remains to be achieved. Dynamic properties of PBA/H_2SO_4 solutions could also be extracted by means of bidimensional and microimaging NMR methods focusing on the solvent ^{1}H resonance, whose behavior suggested that it is influenced only weakly by the alignment of the solute macromolecules.

Besides the potential physicochemical relevance of these conclusions, the present NMR-based results could have implications regarding the ways in which alignment would have to be controlled upon processing a liquid crystalline dope in an industrial setting. Before being able to generalize the PBA conclusions, however, it is important to investigate how widespread are the properties that have been here measured throughout the remainder of the aramide family. When compared with the behavior that has recently been reported for PPTA/H_2SO_4,[27] the similarities between PBA and PPTA are significant. Furthermore, even though the ^{13}C NMR spectra of these two polymers are different because of their different chemical structures, the actual S_{zz}^{o} values observed for both samples are almost identical. The H_2SO_4 ^{1}H NMR spectra of the two polymer solutions are also barely distinguishable, both in their static shift parameters and in their dynamic characteristics. It is important to elucidate whether these coincidences are fortuitous or whether they represent an underlying unity within the aramide family. The second of these possibilities would not only allow further research on the behavior of aramides using simple derivatives such as PBA but would also make superfluous certain searches of enhanced order based on chemical manipulations of the monomeric units. We are consequently expanding our ^{13}C NMR order determinations to a wider class of aramides as well as to an extended range of

concentrations and molecular weights; we trust that these studies will also help us to better understand the discrepancies that remain between the experimentally observed order parameters and those predicted by rigid-rod theories.

Acknowledgment. We are grateful to Dr. John Harwood (University of Illinois-Chicago) for his assistance in recording the 4.7 and 9.4 T NMR data. The present research was supported by the National Science Foundation through grants DMR-9420458 and CHE-9502644 (CAREER Award); L.F. is a Beckman Young Investigator (1996−1998), University of Illinois Junior Scholar (1997−2000), Alfred P. Sloan Fellow (1997−2000), and Camille Dreyfus Teacher-Scholar (1996−2001).

References and Notes

(1) Samulski, E. T. *Phys. Today* **1982**, *35*, 40.
(2) *Polymer Liquid Crystals*; Ciferri, A., Krigbaum, W. R., Meyer, R. B., Eds.; Academic Press: New York, 1982.
(3) *Liquid Crystal Polymers*; Gordon, M.; Cantou, H., Eds.; *Advances in Polymer Science*; 1984; Vols. 59−61.
(4) *Recent Advances in Liquid Crystalline Polymers*; Chapoy, L. L., Ed.; Elsevier: London, 1985.
(5) Finkelmann, H. *Angew. Chem., Int. Ed. Engl.* **1987**, *26*, 816.
(6) Odijk, T. *Macromolecules* **1986**, *19*, 2313.
(7) Northolt, M. G.; Sikkema, D. J. *Adv. Polym. Sci.* **1990**, *98*, 115.
(8) Sato, T.; Teramoto, A. *Adv. Polym. Sci.* **1996**, *126*, 85.
(9) *Liquid Crystalline Polymer Systems*; Isagev, A. I., Kyu, T., Cheng, S. Z. D., Eds.; American Chemical Society: Washington, 1996.
(10) Bair, T. I.; Morgan, P. W.; Killian, F. L. *Macromolecules* **1977**, *10*, 1396.
(11) Kwolek, S. L.; Morgan, P. W.; Schaefgen, J. R.; Gulrich, L. W. *Macromolecules* **1977**, *10*, 1390.
(12) Kwolek, S. L.; Morgan, P. W.; Schaefgen, J. R. In *Encyclopedia of Polymer Science and Engineering*; Wiley: New York, 1988; Vol. 9, Chapter 1.
(13) Yang, H. H. *Aromatic High-Strength Fibers*; Wiley: New York, 1989.
(14) Papkov, S. P.; Kulichikhin, V. G.; Kalmikova, V. G.; Malkin, A. Y. *J. Polym. Sci., Polym. Phys. Ed.* **1974**, *12*, 1753.
(15) Schaefgen, J. R.; Foldi, V. S.; Logullo, F. M.; Good, V. H.; Gulrich, L. W.; Killian, F. L. *Polym. Prepr. (Am. Chem. Soc., Div. Polym. Chem.)* **1976**, *17*, 69.
(16) Panar, M.; Beste, L. F. *Macromolecules* **1977**, *10*, 1401.
(17) Balbi, C.; Bianchi, E.; Ciferri, A.; Tealdi, A.; Krigbaum, W. R. *J. Polym. Sci., Polym. Phys. Ed.* **1980**, *18*, 2037.
(18) Sartirana, M. L.; Marsano, E.; Bianchi, E.; Ciferri, A. *Macromolecules* **1986**, *19*, 1176.
(19) Papkov, S. P.; Iovleva, M. M.; Ivanova, N. A.; Andreyeva, I. N.; Kalmykova, V. D.; Volokhina, A. V. *Polym. Sci. USSR* **1979**, *20*, 742.
(20) Lin, J.; Li, S. *Eur. Polym. J.* **1994**, *30*, 671.
(21) *NMR of Liquid Crystals*; Emsley, J. W., Ed.; Reidel Publishers: Dordrecht, 1985.
(22) Kwolek, S. L. U.S. Patent 3,819,587, 1974.
(23) Sanders, J. K. M.; Hunter, B. K. *Modern NMR Spectroscopy*; Oxford University Press: Oxford, U.K., 1994.
(24) Zhou, M.; Frydman, L. *Solid State NMR* **1995**, *4*, 301.
(25) Pines, A.; Gibby, M. G.; Waugh, J. S. *J. Chem. Phys.* **1973**, *59*, 569.
(26) Frydman, L.; Chingas, G. C.; Lee, Y. K.; Grandinetti, P. J.; Eastman, M. A.; Barrall, G. A.; Pines, A. *J. Chem. Phys* **1992**, *97*, 4800.
(27) Zhou, M.; Frydman, V.; Frydman, L. *J. Phys. Chem.* **1996**, *100*, 19280.
(28) Picken, S. J. *Macromolecules* **1989**, *22*, 1766.
(29) Rommel, H.; Forster, G. *Macromolecules* **1994**, *27*, 4570.
(30) deGennes, P. G. *The Physics of Liquid Crystals*; Clarendon: Oxford, U.K., 1974.
(31) Haeberlen, U. In *Advances in Magnetic Resonance*; Suppl. 1, Waugh, J. S., Ed.; Accademic Press: New York, 1976.
(32) Facelli, J. C.; Grant, D. M. In *Topics in Stereochemistry*; Eliel, E., Wilen, S. H., Eds.; Wiley: New York, 1989; p 1.
(33) Tadokoro, H. *Structure of Crystalline Polymers*; Wiley: New York, 1979.
(34) Schmidt-Rohr, K.; Spiess, H. W. *Multidimensional Solid-State NMR and Polymers*; Academic Press: London, 1994.
(35) Bax, A.; Szeverenyi, M.; Maciel, G. E. *J. Magn. Reson.* **1983**, *52*, 147.
(36) Zeigler, R. C.; Wind, R. A.; Maciel, G. E. *J. Magn. Reson.* **1988**, *79*, 299.
(37) Tycko, R.; Dabbagh, G.; Mirau, P. A. *J. Magn. Reson.* **1989**, *85*, 265.
(38) Gan, Z. H. *J. Am. Chem. Soc.* **1992**, *114*, 8307.
(39) Frydman, L.; Chingas, G. C.; Lee, Y. K.; Grandinetti, P. J.; Eastman, M. A.; Barrall, G.; Pines, A. *Isr. J. Chem.* **1992**, *32*, 161.
(40) Opella, S. J.; Frey, M. G.; Cross, T. A. *J. Am. Chem. Soc.* **1979**, *101*, 5854.
(41) Alemany, L. B.; Grant, D. M.; Pugmire, R. J.; Agler, T. D.; Zilm, K. W. *J. Am. Chem. Soc.* **1983**, *105*, 2133.
(42) Martire, D. E. In *The Molecular Physics of Liquid Crystals*; Luckhurst, G. R., Gray, G. W., Eds.; Academic Press: New York, 1979; p 239.
(43) Due to a typing error the ΔH and ΔS values reported in ref 27 are a factor of 10 smaller than the actual parameters derived from experiments. The correct values for PPTA are $\Delta H = -(17 \pm 1)$ kcal·mol^{-1}, $\Delta S = -(47 \pm 5)$ cal·K^{-1}·mol^{-1}.
(44) Jeener, J.; Meier, B. H.; Bachmann, P.; Ernst, R. R. *J. Chem. Phys.* **1979**, *71*, 4546.
(45) Forsén, S. H.; Hoffman, R. A. *J. Chem. Phys.* **1963**, *39*, 2892.
(46) Forsén, S. H.; Hoffman, R. A. *J. Chem. Phys.* **1964**, *40*, 1189.
(47) Stejskal, E. O.; Tanner, J. E. *J. Chem. Phys.* **1965**, *42*, 288.
(48) Callaghan, P. T. *Principles of Nuclear Magnetic Resonance Microscopy*; Oxford University Press: Oxford, U.K., 1991.
(49) Maier, W.; Saupe, A. *Z. Naturforsch.* **1959**, *14A*, 882.
(50) Maier, W.; Saupe, A. *Z. Naturforsch.* **1960**, *15A*, 287.
(51) Luckhurst, G. R. In *The Molecular Physics of Liquid Crystals*; Academic Press: New York, 1979; p 85.
(52) Beckman, P. A.; Emsley, J. W.; Luckhurst, G. R.; Turner, D. L. *Mol. Phys.* **1986**, *59*, 97.
(53) Fan, S. M.; Luckhurst, G. R.; Picken, S. J. *J. Chem. Phys.* **1994**, *101*, 3255.
(54) Onsager, L. *Ann. N. Y. Acad. Sci.* **1949**, *51*, 627.
(55) Lee, S.-D.; Meyer, R. B. *J. Chem. Phys.* **1986**, *84*, 3443.
(56) Flory, P. J. *Proc. R. Soc. London* **1956**, *A234*, 73.
(57) Flory, P. J. *Adv. Polym. Sci.* **1984**, *59*, 1.
(58) Flory, P. J.; Ronca, G. *Mol. Cryst. Liq. Cryst.* **1979**, *59*, 311.
(59) Papkov, S. P. *Adv. Polym. Sci.* **1984**, *59*, 75.
(60) Tsevtkov, V. N. *Vysokomol. Soedin.* **1977**, *A19*, 2171.
(61) Abe, A.; Yamazaki, T. *Macromolecules* **1989**, *22*, 2138.
(62) Miyajima, S.; McDowell, A. F.; Cotts, R. M. *Chem. Phys. Lett.* **1993**, *212*, 277.
(63) Bitsanis, I.; Davis, H. T.; Tirrell, M. *Macromolecules* **1988**, *21*, 2824.
(64) Bitsanis, I.; Davis, H. T.; Tirrell, M. *Macromolecules* **1990**, *23*, 1157.

MA970233J